Biosensors and Bioelectronics 145 (2019) 111703

Contents lists available at ScienceDirect

Biosensors and Bioelectronics

journal homepage: www.elsevier.com/locate/bios

Polarity inversion sensitized G-quadruplex metal sensors with K^+ tolerance

Ting Ye, Heng Gao, Qingqing Zhang, Chenxiao Yan, Yali Yu, Yifan Fei, Longlong Gao, Xiaoshun Zhou, Yong Shao*

Key Laboratory of the Ministry of Education for Advanced Catalysis Materials, Institute of Physical Chemistry, College of Chemistry and Life Sciences, Zhejiang Normal University, Jinhua, 321004, Zhejiang, China

ARTICLE INFO

Keywords:
G-quadruplex
Polarity inversion
K^+ tolerance
Hypericin
Metal sensor
Fluorescence

ABSTRACT

Due to the high abundance of K^+ in environments and K^+-induced high stability of G-quadruplex (G4), developing a selective G4-based fluorescent sensor for other metal ions with K^+ tolerance is a great challenge. Herein, we found that even in the presence of 15000-fold excess of K^+, Ba^{2+} exhibits a highly specific binding with a human telomeric G4 (htG4) in comparison with other G4-binding metal ions such as Pb^{2+} and Sr^{2+}. This specific binding event can be recognized by a natural fluorophore of hypericin with a lighting-up fluorescence response. Interestingly, inverting the polarity of the most 3' G in htG4 can sensitize the Ba^{2+} response with the retaining Ba^{2+} specificity and K^+ tolerance. This polarity inversion of htG4 causes a G4 conformation change in K^+ and the polarity-inverted htG4 tends to favorably dimerize in response to the Ba^{2+} specific binding. To our knowledge, this is the first report that polarity inversion of G4 can be applied to construct a selective metal sensor with K^+ tolerance. Our findings will open a new way to conveniently regulate the G4 conformation and stability by polarity inversion towards developing high-performance sensors.

1. Introduction

Guanine-rich nucleic acids have potentials to form stable G-quadruplex (G4) structures with assistance of specific metal ions. This provides an excellent platform for developing G4-based metal sensors (Zhou et al., 2017). Especially, K^+ having a matchable size and low dehydration energy in inserting between adjacent quartets exhibits a preferable G4 binding specificity with respect to other monovalent ions of Li^+, Na^+, Rb^+, and Cs^+ (Ida and Wu, 2008; Vummidi et al., 2013; Bhattacharyya et al., 2016; Hud et al., 1996). Various G4-based K^+ sensors have been successfully developed using fluorescence, colorimetry, and electrochemistry signals as readouts (Liu et al., 2014; Qin et al., 2010; Yang et al., 2016; Zhang et al., 2016a; Li et al., 2010; He et al., 2005; Ueyama et al., 2002; Wu et al., 2017; Wang et al., 2006). The undesired G4 binding of other multivalent metal ions can be avoided by addition of strong masking reagents like EDTA. However, several ions including Pb^{2+}, Ba^{2+}, Sr^{2+}, NH_4^+, Cu^{2+}, Ca^{2+}, and Tl^+ have been reported to have a G4 binding strength comparable to or even higher than K^+ (Wang et al., 2012; Liu et al., 2012; Li et al., 2009; Patil and Rhodes, 2000; Zavyalova et al., 2016; Kankia and Marky, 2001; Vairamani and Gross, 2003; Shi et al., 2001) and several G4-based metal sensors have been developed (Lin et al., 2017; Yang et al., 2013; Leung et al., 2012; He et al., 2013; Hoang et al., 2016; Kotch et al., 2000; Xu et al., 2017). The ionic radii, metal-oxygen binding strength, electrostatic interaction, hydration energy, etc. are believed to be the crucial factors to determine the metal affinity (Vairamani and Gross, 2003; Deepa et al., 2011; Miserachs et al., 2016; Sravani et al., 2011). Two concerns should be addressed in developing an ideal sensor for these metal ions. Firstly, since K^+ is abundant in living cells and environments and is difficult to be removed out from samples by common masking reagents, the K^+ tolerance must be met in developing G4-based sensors for these metals. Usually, specific sequences are required to fold into G4 structures with association of these metal ions at micromole concentration, while these methods cann't tolerate K^+ at millimole concentration. Secondly, rational strategies are needed to differentiate metal ions of interest from others that also have a strong G4 binding. For example, Sr^{2+} and Ba^{2+} exhibit affinity higher than K^+ in binding with thrombin binding aptamer G4 (TBA) (Kankia and Marky, 2001). However, developing a selective G4-based Ba^{2+} sensor is still a great challenge since Sr^{2+} even has a stronger G4 binding than Ba^{2+} for some G4 structures (Kwan et al., 2011; Kankia and Marky, 2001; Sravani et al., 2011; Seo et al., 2012). Although Ba^{2+} has an ion radii and dehydration energy that are not significantly different from K^+ and also prefers to bind in-between G tetrads (Kankia and Marky, 2001; Pan et al., 2003; Zhang et al., 2014), its binding specificity with G4 at excess of K^+ has not been explored (Bhattacharyya et al., 2016;

* Corresponding author.
E-mail address: yshao@zjnu.cn (Y. Shao).

https://doi.org/10.1016/j.bios.2019.111703
Received 27 July 2019; Received in revised form 5 September 2019; Accepted 13 September 2019
Available online 15 September 2019
0956-5663/ © 2019 Elsevier B.V. All rights reserved.

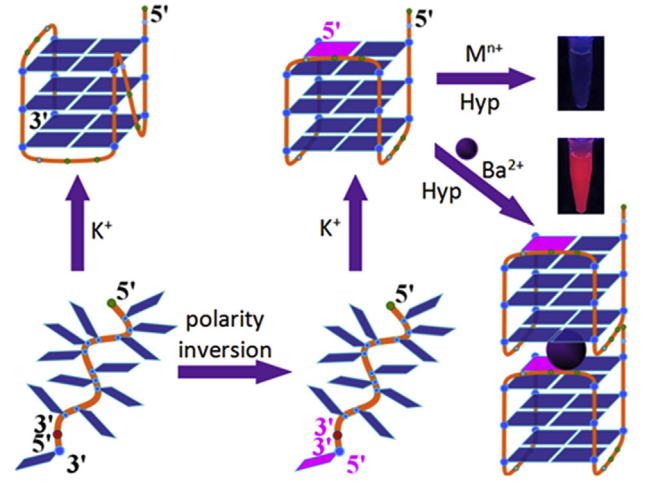

Name	Sequence
TAQ	5'-TAGGGTTAGGGTTAGGGTTAGGG-3'
TAQ-3iG	5'-TAGGGTTAGGGTTAGGGTTAGG-3'-3'-G-5'
TAQ-5iG	5'-TA-3'-3'-G-5'-5'-GGTTAGGGTTAGGGTTAGGG-3'
TAQ-5iTAG	3'-TAG-5'-5'-GGTTAGGGTTAGGGTTAGGG-3'

Scheme 1. Polarity inversion induced G4 conformation change and sensitized Ba^{2+} response. Also shown are the primary G4 sequences used in this work.

Miserachs et al., 2016). Furthermore, the allowed Ba^{2+} content in drinking water is less than 5 μM (GB5749-2006 in China) that is much higher for Pb^{2+} (70 nM) and lower for Sr^{2+} (46 μM) (Zhou et al., 2017; Qu et al., 2012). Thus, a selective recognition of Ba^{2+} over Sr^{2+} and other common ions is greatly demanded for practical applications.

Herein, we made an effort to develop a selective G4-based Ba^{2+} sensor with excellent tolerance to highly-concentrated K^+ and without interference from other G4-binding ions including Sr^{2+} and Pb^{2+}. Hypericin (Hyp) was selected as the fluorescent probe since its optical property is dependent on the G4 sequences and structures (Lin et al., 2017; Zhang et al., 2016b).

2. Materials and methods

2.1. Reagents and chemicals

Metal salts were purchased from Aladdin Reagent Co. (Shanghai, China). Hypericin (Hyp) was provided by Yuanye Technology Co. Ltd (Shanghai, China). DNA oligonucleotides (Scheme 1 in text and Table S1) were synthesized by TaKaRa Biotechnology Co., Ltd (Dalian, China) and purified by HPLC. The nucleic acid concentrations were measured by first dissolving DNA in pure water and detecting the UV absorbance at 260 nm using extinction coefficients calculated by nearest neighbor analysis. Other reagents were of analytical grade (Sigma Chemical Co., St. Louis, USA) and used without any purification. Milli-Q water (18.2 MΩ; Millipore Co, Billerica, USA) was used in all of the experiments.

2.2. Fluorescence measurements

Fluorescence spectra were acquired with a FLSP920 spectrofluorometer (Edinburgh Instruments Ltd., Livingston, UK) at 20 °C, which was controlled by a temperature-controlled circulator (Julabo Labortechnik GmbH, Seelbach, Germany). Fluorescence was measured in a quartz cell with path length of 1 cm with excitation at 466 nm. To prepare the nucleic acid solution with a thermodynamically stable conformation, the nucleic acid strand was annealed in K^+ in a thermocycler (first at 92 °C, then slowly cooled to room temperature) and stored in 4 °C overnight. The resultant solution was then incubated with the specified metal ion for 30 min. Finally, Hyp at the specified concentration was added into the nucleic acid solution, and the resulting solution allowed incubation for 30 min before fluorescence measurements. Phosphate buffer (7 mM, pH 7.2) containing 60 mM K^+ (PBS) was optimized as the preferable buffer for the binding specificity of Ba^{2+} over other metal ions. The fluorescence experiments were at least triplicated and the deviation in fluorescence measurements of Hyp was less than 7%.

The G4 binding stoichiometries with Hyp and Ba^{2+} were determined using the Job's plot method. The total concentration of the involved species was maintained at 2 μM. To ensure reliability of the Job's plot analysis by fluorescence, Hyp at 10 μM far in excess of G4 was used to proportionally index the formed Ba^{2+}-G4 complex in evaluating the Ba^{2+} binding stoichiometry with G4, while the concentration ratio of Ba^{2+} to G4 held at 5:1 to proportionally index the formed Hyp-G4 complex in evaluating the Hyp binding stoichiometry with G4. The binding stoichiometries were measured by the cross point of two tangent lines in the ranges of fluorescence increase and decrease stages.

2.3. DNA melting temperature (T_m) measurements

The melting temperatures (T_m) of G4s in the absence and presence of Ba^{2+} were determined using a UV2550 spectrophotometer (Shimadzu Corp., Kyoto, Japan), equipped with a TMSPC-8 T_m analysis system. The absorbance of G4 at 295 nm as a function of the solution temperature between 5 °C and 90 °C was collected in 0.5 °C increment, with a ramp rate of 2 °C/min and a 30-s equilibration time applied after each temperature increment. To avoid the effect of possible hydrolysis of metal ions on the T_m measurements, 7 mM PBS buffer containing 60 mM K^+ but at pH 5.3 was used.

2.4. Circular dichroism (CD) spectra measurements

CD spectra were measured on a MOS-500 CD spectrometer (Bio-Logic Science Instruments, France) using a 2-mm path-length quartz cell. Scans were performed at a temperature-controlled holder (20 °C) over a wavelength range of 200–400 nm with a scanning speed of 200 nm/min and 1 nm pitch. Buffer blank was subtracted from the collected data. The given CD spectra were three scans averaged and zero-corrected at 400 nm.

2.5. ITC measurements

Isothermal titration calorimetry (ITC) measurements were carried out at 20 °C using an ITC200 microcalorimeter (MicroCal, LLC, Northampton, MA). In 10 mM Tris-HCl buffer (pH 7.2) containing 0.5 mM K^+ (in this buffer, a large ITC signal can be obtained), G4 (10 μM) in the sample cell was droppingly titrated using 2 μL of 100 μM Ba^{2+} (the first 0.4 μL injection was followed by 19 injections of 2 μL with 20s duration at 150s time intervals). The titration of Ba^{2+} in the syringe into the identical buffer solution in the sample cell without DNA was used as a control to obtain the dilution heat. Origin (version 7.0) software was used for data analysis. The area of each injection peak was automatically integrated. A binding isothermal curve was obtained by plotting the total heat per injection (kcal mol^{-1} of injectant) as a function of the molar ratio of Ba^{2+} to G4.

2.6. Sample analysis

Due to toxicity of Ba^{2+} in drinking water, commercially bottled mineral water was used as the typical sample to confirm the feasibility of our method. Ba^{2+} was added into the sample to test the recovery. The sample was first treated with 7 mM PBS buffer (pH 7.2) to remove potential heavy metal ions by centrifugation due to their precipitation interaction with phosphate anion. 100 nM Ba^{2+} (final concentration in the measuring solution) was added into the sample and pretreated using

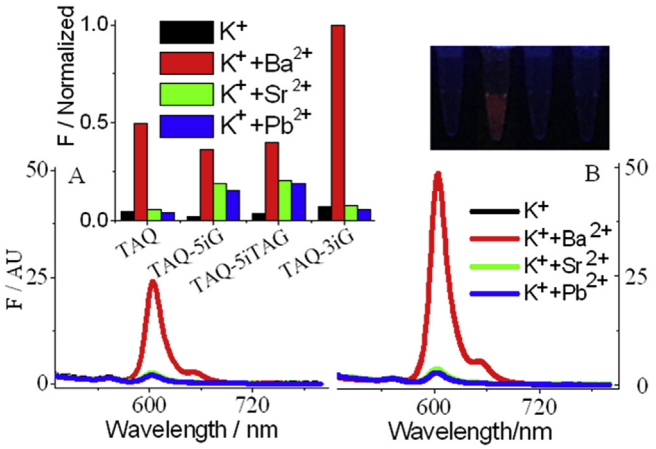

Fig. 1. Fluorescence emission spectra of Hyp (4 μM) in 7 mM PBS buffer (pH 7.2) containing 60 mM K^+ and (A) TAQ, (B) TAQ-3iG (1 μM) in the absence and presence of Ba^{2+}, Sr^{2+}, and Pb^{2+} (4 μM), respectively. Excitation: 466 nm. Inset: (left) Dependence of the Hyp fluorescence at 603 nm on TAQ, TAQ-3iG, TAQ-5iG, and TAQ-5iTAG; (right) Photographs of the Hyp-TAQ-3iG solutions in the absence and presence of Ba^{2+}, Sr^{2+}, and Pb^{2+}, respectively under UV illumination (from left to right).

the same procedure. Fluorescence was measured in 7 mM PBS buffer (pH 7.2) containing 60 mM K^+, 1 μM TAQ-3iG, 4 μM Hyp. The added Ba^{2+} was measured by the primarily established work curve.

3. Results and discussion

3.1. Ba^{2+} specificity in lighting-up the Hyp-G4 fluorescence and the polarity inversion sensitized response

We first investigated the fluorescence response of Hyp in binding with a human telomeric G4 (htG4) sequence of TAQ (Scheme 1) in PBS. As shown in Fig. 1A, in this case, Hyp is weakly fluorescent regardless of this G4 existence, as confirmed by our previous report (Lin et al. 2017). However, further addition of 4 μM Ba^{2+} (15000-fold lower than K^+ in concentration) brings an 11-fold increase in the Hyp fluorescence, whereas Sr^{2+} and Pb^{2+} at the same concentration make Hyp emitting still at the background level. Since it has been reported that the Hyp fluorescence is dependent on the G4 conformation, thus Ba^{2+} should cause a change in the TAQ conformation from the original hybrid-1 structure (Wu et al., 2017) to the one suitable for Hyp binding. Note that this is the first report for a G4-based metal ion specificity that can tolerate highly-concentrated K^+. We then tested effect of other G4 sequences (Table S1) and conformations (including hybrid-1, hybrid-2, anti-parallel, and parallel) on lighting up the Hyp fluorescence in response to the Ba^{2+} addition. As shown in Fig. S1, it seems that htG4s that adopt hybrid conformations are more sensitive in fluorescence response to Ba^{2+} in comparison with other sequences and conformations, in which TAQ is an efficient G4 sequence. Since the fluorescence response is likely independent of the hybrid-1 and hybrid-2 conformations, as evidenced by the AP7 and AP19 htG4 that dominantly adopt both conformations by introduction of an abasic site (Table S1 and Fig. S1) (Wu et al. 2017), the observed robust dependence of Hyp fluorescence on the variant 3' and 5' terminal sequences of htG4s (Fig. S1) suggests that these terminal sequences also regulate the Ba^{2+} binding. For example, relative to TAQ with 5'-TA-3' dinucleotide at the 5' end of the htG4, removing the most 5' T mononucleotide (thus giving AQ, Table S1) and lengthening a most 3' T mononucleotide (thus giving TAQT, Table S1) subsequently bring 2.4- and 3-fold lower Hyp fluorescence in response to Ba^{2+}, likely suggesting that Ba^{2+} leads to a htG4 conformation modification or an assembled structure (Zavyalova et al. 2016; Lu et al. 2015).

We then tried to sensitize the Hyp fluorescence response to Ba^{2+}. It has been reported that inversion of the trinucleotide polarity of 5'-GGT-3' locating in the 5' terminal of TBA to 3'-GGT-5' leads to another well-defined G4 structure (mTBA, Table S1) with distinct guanine syn-/anti-orientations (Martino et al. 2006). Unfortunately, mTBA exhibits a weaker fluorescence response to Ba^{2+} in comparison with TBA (Fig. S1). Herein, we likewise inverted the TAQ polarities at the 5' most terminal G mononucleotide and TAG trinucleotide, and the 3' most terminal G mononucleotide to give TAQ-5iG, TAQ-5iTAG, and TAQ-3iG (Scheme 1), respectively. Interestingly, TAQ-5iG and TAQ-5iTAG display a fluorescence decrease in the Ba^{2+} response specificity over Sr^{2+} and Pb^{2+}, whereas TAQ-3iG holds the Ba^{2+} specificity but otherwise with a sensitized fluorescence response that is two-fold brighter than TAQ does (Fig. 1B and inset). The differentiation of Ba^{2+} from Sr^{2+} and Pb^{2+} can be visualized by the red appearance of only the Ba^{2+} solution under UV illumination. We found that PBS buffer with highly-concentrated K^+ strongly favor the fluorescence specificity to Ba^{2+} over Pb^{2+} and Sr^{2+} (Fig. S2) mostly because of their differences in the phosphate binding behaviors and dehydration energies (Seo et al. 2012). We have proved that a suitable G4 construct can tear apart the Hyp non-fluorescent aggregates to bring the fluorescent monomer (we named dispersion-induced fluorophore (DIF)) (Lin et al. 2017). Therefore, Ba^{2+} can heavily regulate the TAQ-3iG structure to favor the Hyp binding with an efficient DIF effect.

3.2. Thermodynamic characterization of the Ba^{2+} binding specificity with G4s

To confirm the Ba^{2+} binding specificity with TAQ-3iG, the absorbance at 295 nm as a function of solution temperature was measured. As shown in Fig. 2A, the absorbance of 4 μM TAQ-3iG in 60 mM K^+ decreases upon increasing the solution temperature with a T_m value at about 51.8 °C, suggesting formation of a G4 structure in spite of the polarity inversion. However, addition of equivalent Ba^{2+} (4 μM) abruptly shifts the T_m value to 65.4 °C, whereas Sr^{2+} and Pb^{2+} exhibit no effect on the TAQ-3iG melting behavior. Furthermore, the T_m value doesn't change significantly with the Ba^{2+} concentration higher than 4 μM (Fig. 2B). This suggests a high binding specificity of Ba^{2+} with TAQ-3iG, as observed in Fig. 1. For comparison, the T_m values of TAQ, TAQ-5iG, and TAQ-5iTAG in 60 mM K^+ were also measured (Fig. S3 for melting curves) to be about 62.8, 68.8, and 62.7 °C (Fig. 2C), respectively. Thus, inverting the polarity of the 3' most terminal G mononucleotide in TAQ significantly destabilizes the G4 structure with

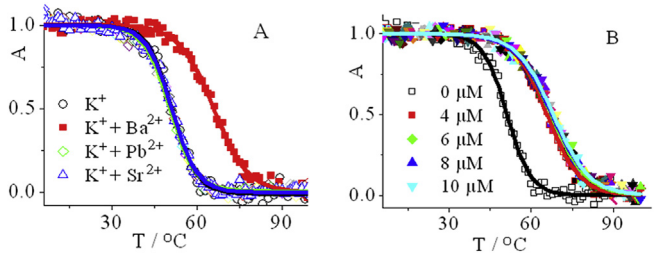

C

	Ba^{2+} free	4 μM Ba^{2+}	△T
TAQ	62.8	71.4	8.6
TAQ-3iG	51.8	65.4	13.6
TAQ-5iG	68.8	78.3	9.5
TAQ-5iTAG	62.7	71.6	8.8

Fig. 2. (A) Melting curves of TAQ-3iG (4 μM) in 7 mM PBS buffer (pH 5.3) containing 60 mM K^+ in the absence and presence of Ba^{2+}, Sr^{2+}, and Pb^{2+} (4 μM). (B) Melting curves of TAQ-3iG (4 μM) in 7 mM PBS buffer (pH 5.3) containing 60 mM K^+ with Ba^{2+} at 0, 4, 6, 8, and 10 μM, respectively. The absorbance at 295 nm was measured and normalized. (C) The fitted Tm values of G4s (4 μM) in the absence and presence of Ba^{2+} (4 μM).

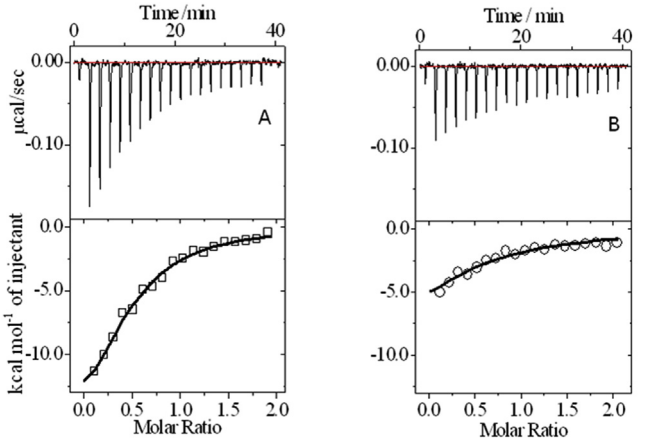

	n site	K 10^5/M	△H kcal/mol	△S cal/mol/deg	△G kcal/mol
A	0.48(±0.04)	3.43(±0.49)	-19.5(±1.97)	-41.2	-7.43
B	0.52(±0.01)	1.09(±0.15)	-13.6(±0.90)	-23.5	-6.75

Fig. 3. Binding of Ba^{2+} with TAQ-3iG evaluated by ITC. TAQ-3iG (A) and TAQ (B) at 10 μM were separately titrated by 100 μM Ba^{2+} in 10 mM Tris-HCl buffer (pH 7.2) containing 0.5 mM K^+ at 20 °C. Inset table: the thermodynamic fitting results.

respect to other polarity-inverted cases. On the other hand, addition of Ba^{2+} otherwise brings the largest T_m change (ΔT_m) for TAQ-3iG in comparison with TAQ, TAQ-5iG, and TAQ-5iTAG (13.6 versus 8.6, 9.5, and 8.8 °C in ΔT_m, Fig. 2C). Note that at higher Ba^{2+} concentration, the thermal stability change of TAQ always falls below that of TAQ-3iG (Fig. S4), further suggesting the crucial role of polarity inversion in strengthening the Ba^{2+} binding affinity. We found that the T_m value of TAQ-3iG in the presence of Ba^{2+} is dependent on the G4 concentration (Fig. S5), suggesting formation of an intermolecular G4 assembly (Kaushik et al. 2007).

Isothermal titration calorimetry (ITC) was then used to evaluate the Ba^{2+} binding with TAQ and TAQ-3iG (Fig. 3). Interestingly, we found that Ba^{2+} seems to bind with these G4s in a 1:2 mode, whereas the binding affinity of Ba^{2+} with TAQ-3iG is three-fold higher than with TAQ, suggesting the significant role of the polarity inversion in strengthening the G4 binding. Thus, the intermolecular G4 dimer assembly induced by Ba^{2+} is expected to favor the Hyp binding. The 1:2 binding mode of Ba^{2+} with TAQ-3iG and TAQ was also confirmed by Job's plot analysis (Fig. S6). The smaller binding enthalpy (△H) and entropy (△S) of Ba^{2+} with TAQ-3iG demonstrate a preferred specific binding of Ba^{2+} *via* an intermolecular G4 assembly. On the other hand, according to Job's plot analysis (Fig. S7), the binding of Hyp with TAQ-3iG and TAQ in the presence of Ba^{2+} follows a 1:1 mode (because of Hyp aggregation (Lin et al. 2017), this mode cannot be precisely evaluated by ITC).

3.3. CD investigation of the G4 conformation upon the Ba^{2+} binding

Circular dichroism spectra (CD) were employed to examine the Ba^{2+} induced G4 restructuring. TAQ in K^+ exhibits a large positive CD band at 289 nm, a shoulder at 276 nm, and a weak negative band at 239 nm, typical of a hybrid-1 G4 structure (Kypr et al. 2009). However, TAQ-3iG clearly displays a positive band at 292 nm, a negative band at 263 nm, and a positive band at 247 nm, showing the role of the 3' G polarity in defining the htG4 conformation (Fig. 4). On the other hand, TAQ-5iG and TAQ-5iTAG display CD bands very similar to TAQ (Fig. S8), indicating that these polarity inversions don't significantly alter the G4 conformation. The CD bands of TAQ-3iG are otherwise in similarity with those of TBA (Fig. S9), suggesting that TAQ-3iG adopts a chair

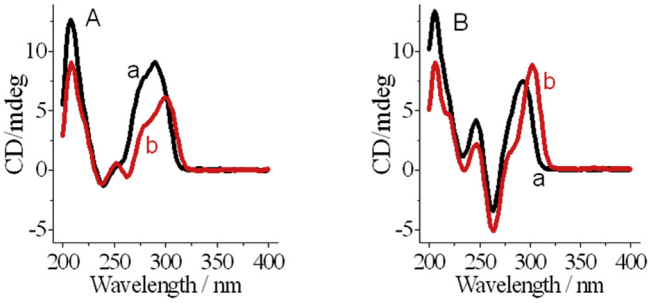

Fig. 4. CD spectra of (A) TAQ and (B) TAQ-3iG (8 μM) in the (a) absence and (b) presence of Ba^{2+} (40 μM) in PBS buffer (pH 7.2, 60 mM K^+) at 20 °C.

anti-parallel G4 structure. This is the first report on the htG4 conformation changes caused by the polarity inversion. However, addition of Ba^{2+} to the TAQ solution alters the CD bands a little towards those of TAQ-3iG alone in K^+, showing the Ba^{2+} capability in regulating the htG4 structure. More interestingly, Ba^{2+} not only enhances the CD band of TAQ-3iG at 263 nm, but also causes a significant red shift of the broad band at 292 nm to subsequently give a narrow band at 302 nm, demonstrating an enhanced exciton coupling as a result of the Ba^{2+}-induced dimer assembly of TAQ-3iG (Masiero et al. 2010), most possibly analogous to the sandwich structure (Shi et al. 2001; Zhang et al. 2014). Since Ba^{2+} at micromole concentration binds with TAQ and TAQ-3iG that have three tetrad planes in a 1:2 mode in the presence of excess of K^+, it is expected that the intermolecular G4 binding of Ba^{2+} (Scheme 1), not the intramolecular binding, causes the observed CD changes.

3.4. Ba^{2+} selectivity over other metal ions and sample analysis

To get the sensitizing competency of the polarity inversion, the metal ion concentration-dependent response was checked. As demonstrated in Fig. 5A, both TAQ and TAQ-3iG exhibit a highly selective fluorescence response to Ba^{2+} in contrast to the non-fluorescent response to Sr^{2+} and Pb^{2+}. However, TAQ-3iG otherwise exhibits a remarkably sensitized response slope that is 3.7 times higher than TAQ in the initially investigated Ba^{2+}concentration range, while at excess of

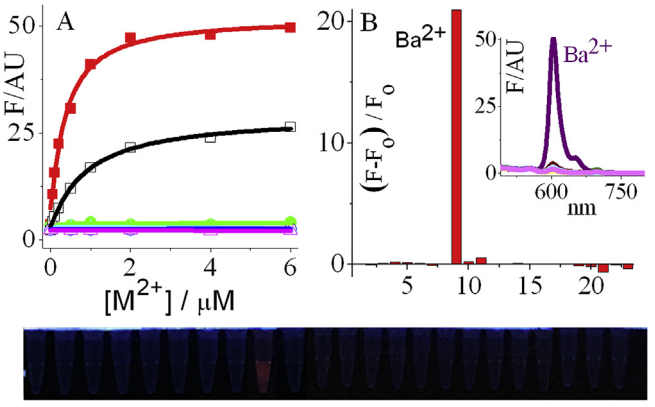

Fig. 5. (A) Fluorescence response of Hyp (4 μM) in 7 mM PBS (pH 7.2, 60 mM K^+) containing 1 μM TAQ-3iG (solid symbol) and TAQ (open symbol) to Ba^{2+} (square), Sr^{2+} (circle), and Pb^{2+} (triangle), respectively. (B) Selective response of TAQ-3iG to metal ions (from 1 to 23: blank, 1000 μM Li^+, Na^+, K^+, Rb^+, Cs^+, Mg^{2+}, Ca^{2+}; 4 μM Sr^{2+}, Ba^{2+}; 10 μM Hg^{2+}, Ag^+, Al^{3+}, In^{3+}, Cd^{2+}, Mn^{2+}, Cr^{3+}, Fe^{3+}, Co^{2+}, Ni^{2+}, Cu^{2+}, Zn^{2+}, Pb^{2+}). F_0 and F stand for the fluorescent intensities in the absence and presence of metal ion. Inset: the corresponding emission spectra. (C) Photographs of these metal ion solutions under UV illumination (from left to right). The red appearance corresponds to the Ba^{2+} solution. (For interpretation of the references to color in this figure legend, the reader is referred to the Web version of this article.)

Ba^{2+}, about two times higher fluorescence response is reached for TAQ-3iG in comparison to TAQ. The Ba^{2+} concentration at nM level can be even sensed with the limit of detection of about 4 nM using TAQ-3iG as the element assuming a signal-to-noise ratio of 3 (Fig. S10). These results demonstrate the substantial role of polarity inversion of the 3' G in sensitizing the Ba^{2+} response. Furthermore, the Ba^{2+} selectivity of TAQ-3iG becomes better at pH > 6.0 (Fig. S11). Additionally, other common metal ions including Li^+, Na^+, Rb^+, Cs^+, Mg^{2+}, Ca^{2+}, Hg^{2+}, Ag^+, Al^{3+}, In^{3+}, Cd^{2+}, Mn^{2+}, Cr^{3+}, Fe^{3+}, Co^{2+}, Ni^{2+}, Cu^{2+}, and Zn^{2+} exhibit no fluorescence response (Fig. 5B). Especially, Mg^{2+} and Ca^{2+} that belong to the same main group elements as Ba^{2+} in the Periodic Table still hold a silent fluorescence reponse even with their concentrations 250-fold higher than Ba^{2+}. Furthermore, although Sr^{2+} has been reported to have a strong binding with G4 (Kwan et al. 2011; Kankia and Marky, 2001; Sravani et al. 2011; Seo et al. 2012), we found that coexistence of Sr^{2+} with its concentration till up to 1000 μM has a negligible effect on the fluorescence response of TAQ-3iG to 4 μM Ba^{2+} in our condition (Fig. S12). These results prove that the polarity inversion provides a new way to construct a novel sensor with a high sensitivity and selectivity for Ba^{2+} assay. We finally tested several brands of commercially available mineral drinking water samples by conducting a simple pretreatment and standard addition experiments (for the experimental procedures, see the support information), and good recoveries were observed (Table S2), suggesting a promising application of our method in the real sample analysis.

4. Conclusions

In conclusion, Ba^{2+} owns a specific binding with htG4 even in the presence of 15000-fold excess of K^+. The natural Hyp can serve as a lighting-up fluorophore to recognize this binding event. Furthermore, the effect of polarity inversion was investigated and we found that inverting the polarity of the most 3' G can sensitize the Ba^{2+} response with the retained specificity against other metal ions, for example, especially the same main group element of Sr^{2+}. This polarity inversion changes the htG4 folding from the hybrid to the chair anti-parallel conformation and the Ba^{2+} specific binding brings a favorable intermolecular dimer assembly. This is the first report that the G4 polarity inversion can be used to construct a selective sensor with a K^+ tolerance. Our results will open a new way to conveniently regulate the G4 conformation and stability by polarity inversion towards developing novel sensors.

CRediT authorship contribution statement

Ting Ye: Writing - original draft. **Heng Gao:** Methodology. **Qingqing Zhang:** Software. **Chenxiao Yan:** Software. **Yali Yu:** Software. **Yifan Fei:** Writing - original draft. **Longlong Gao:** Writing - review & editing. **Xiaoshun Zhou:** Project administration. **Yong Shao:** Supervision, Funding acquisition.

Declaration of competing interest

The authors declare that they have no known competing financial interests or personal relationships that could have appeared to influence the work reported in this paper.

Acknowledgments

This work was supported by the National Natural Science Foundation of China (Grant No. 21675142 and 21545009).

Appendix A. Supplementary data

Supplementary data to this article can be found online at https://doi.org/10.1016/j.bios.2019.111703.

References

Bhattacharyya, D., Mirihana Arachchilage, G., Basu, S., 2016. Front. Chem. 4, 1–14.
Deepa, P., Kolandaivel, P., Senthilkumar, K., 2011. Comput. Theor. Chem. 974, 57–65.
He, F., Tang, Y., Wang, S., Li, Y., Zhu, D., 2005. J. Am. Chem. Soc. 127, 12343–12346.
He, H., Wang, M., Chan, D.S.-H., Leung, C.-H., Lin, X., Lin, J., Ma, D.-L., 2013. Methods 64, 212–217.
Hoang, M., Huang, P.-J.J., Liu, J., 2016. ACS Sens. 1, 137–143.
Hud, N.V., Smith, F.W., Anet, F.A., Feigon, J., 1996. Biochemistry 35, 15383–15390.
Ida, R., Wu, G., 2008. J. Am. Chem. Soc. 130, 3590–3602.
Kankia, B.I., Marky, L.A., 2001. J. Am. Chem. Soc. 123, 10799–10804.
Kaushik, M., Suehl, N., Marky, L.,A., 2007. Biophys. Chem. 126, 154–164.
Kotch, F.W., Fettinger, J.C., Davis, J.T., 2000. Org. Lett. 2, 3277–3280.
Kwan, I.C.M., She, Y.-M., Wu, G., 2011. Can. J. Chem. 89, 835–844.
Kypr, J., Kejnovská, I., Renčiuk, D., Vorlíčková, M., 2009. Nucleic Acids Res. 37, 1713–1725.
Leung, K.-H., Ma, V.P.-Y., He, H.-Z., Chan, D.S.-H., Yang, H., Leung, C.-H., Ma, D.-L., 2012. RSC Adv. 2, 8273–8276.
Li, T., Wang, E., Dong, S., 2010. Anal. Chem. 82, 7576–7580.
Li, T., Wang, E., Dong, S., 2009. J. Am. Chem. Soc. 131, 15082–15083.
Lin, F., Hu, Y.H., Wu, T., Zhou, X.S., Shao, Y., 2017. Sens. Actuators B Chem. 247, 19–25.
Liu, L., Shao, Y., Peng, J., Huang, C., Liu, H., Zhang, L., 2014. Anal. Chem. 86, 1622–1631.
Liu, W., Zhu, H., Zheng, B., Cheng, S., Fu, Y., Li, W., Lau, T.C., Liang, H., 2012. Nucleic Acids Res. 40, 4229–4236.
Lu, H., Li, S., Chen, J., Xia, J., Zhang, J., Huang, Y., Liu, X., Wu, H.-C., Zhao, Y., Chai, Z., Hu, Y., 2015. Metallomics 7, 1508–1514.
Martino, L., Virno, A., Randazzo, A., Virgilio, A., Esposito, V., Giancola, C., Bucci, M., Cirino, G., Mayol, L., 2006. Nucleic Acids Res. 34, 6653–6662.
Masiero, S., Trotta, R., Pieraccini, S., De Tito, S., Perone, R., Randazzo, A., Spada, G.P., 2010. Org. Biomol. Chem. 8, 2683–2692.
Miserachs, H.G., Donghi, D., Borner, R., Johannsen, S., Sigel, R.K.O., 2016. J. Biol. Inorg. Chem. 21, 975–986.
Pan, B., Xiong, Y., Shi, K., Deng, J., Sundaralingam, M., 2003. Structure 11, 815–823.
Patil, S.D., Rhodes, D.G., 2000. Nucleic Acids Res. 28, 2439–2445.
Qin, H., Ren, J., Wang, J., Luedtke, N.W., Wang, E., 2010. Anal. Chem. 82, 8356–8360.
Qu, K., Zhao, C., Ren, J., Qu, X., 2012. Mol. Biosyst. 8, 779–782.
Seo, J., Hong, E.S., Yoon, H.-J., Shin, S.K., 2012. Int. J. Mass Spectrom. 330, 262–270.
Shi, X., Fettinger, J.C., Davis, J.T., 2001. J. Am. Chem. Soc. 123, 6738–6739.
Sravani, M., Nagaveni, V., Prabhakar, S., Vairamani, M., 2011. Mass Spectrom. 25, 2095–2098.
Ueyama, H., Takagi, M., Takenaka, S., 2002. J. Am. Chem. Soc. 124, 14286–14287.
Vairamani, M., Gross, M.L., 2003. J. Am. Chem. Soc. 125, 42–43.
Vummidi, B.R., Alzeer, J., Luedtke, N.W., 2013. Chembiochem 14, 540–558.
Wang, C., Li, Y., Jia, G., Liu, Y., Lu, S., Li, C., 2012. Chem. Commun. 48, 6232–6234.
Wang, L., Liu, X., Hu, X., Song, S., Fan, C., 2006. Chem. Commun. 36, 3780–3782.
Wu, T., Ye, M.Y., Mao, T.Y., Lin, F., Hu, Y.H., Gan, N., Shao, Y., 2017. Anal. Chim. Acta 964, 161–169.
Xu, L., Chen, Y., Zhang, R., Gao, T., Zhang, Y., Shen, X., Pei, R., 2017. J. Fluoresc. 27, 569–574.
Yang, C., Liu, L., Zeng, T., Yang, D., Yao, Z., Zhao, Y., Wu, H.-C., 2013. Anal. Chem. 85, 7302–7307.
Yang, L., Qing, Z., Liu, C., Tang, Q., Li, J., Yang, S., Zheng, J., Yang, R., Tan, W., 2016. Anal. Chem. 88, 9285–9292.
Zavyalova, E., Tagiltsev, G., Reshetnikov, R., Arutyunyan, A., Kopylov, A., 2016. Nucleic Acid Ther. 26, 299–308.
Zhang, D., Huang, T., Lukeman, P.S., Paukstelis, P.J., 2014. Nucleic Acids Res. 42, 13422–13429.
Zhang, S., Zhang, R., Ma, B., Qiu, J., Li, J., Sang, Y., Liu, W., Liu, H., 2016a. RSC Adv. 6, 41999–42007.
Zhang, X., Jin, B., Zheng, W., Zhang, N., Liu, X., Bing, T., Wei, Y., Wang, F., Shangguan, D., 2016b. Dyes Pigments 132, 405–411.
Zhou, W., Saran, R., Liu, J., 2017. Chem. Rev. 117, 8272–8325.